Accelerated black holes in an anti-de Sitter universe

Pavel Krtouš*
Institute of Theoretical Physics, Faculty of Mathematics and Physics, Charles University in Prague, V Holešovičkách 2, 180 00 Prague 8, Czech Republic

(Version 2.00; 23rd October 2005)

The C-metric is one of few known exact solutions of Einstein's field equations which describes the gravitational field of moving sources. For a vanishing or positive cosmological constant, the C-metric represents two accelerated black holes in asymptotically flat or de Sitter spacetime. For a negative cosmological constant the structure of the spacetime is more complicated. Depending on the value of the acceleration, it can represent one black hole or a sequence of pairs of accelerated black holes in the spacetime with an anti-de Sitter-like infinity. The global structure of this spacetime is analyzed and compared with an empty anti-de Sitter universe. It is illustrated by 3D conformal-like diagrams.

PACS numbers: 04.20.Ha, 04.20.Jb

I. INTRODUCTION

The C-metric without cosmological constant Λ is a well-known solution of the Einstein(-Maxwell) equations. It belongs to a class of spacetimes with boost-rotational symmetry [1] which represent the gravitational field of uniformly accelerated sources. The C-metric was discovered back in 1917 by Levi-Civita [2] and Weyl [3], and named by Ehlers and Kundt [4]. An understanding of the global structure of the C-metric spacetime as a universe with a pair of accelerated black holes came with the fundamental papers by Kinnersley and Walker [5], Ashtekar and Dray [6] and Bonnor [7]. Various aspects and properties of this solution were consequently studied, including the generalization to spinning black holes. References and overviews can be found, e.g., in Refs. [1, 8, 9, 10]; for recent results see, e.g., Refs. [11, 12, 13].

A generalization of the standard C-metric for nonvanishing cosmological constant Λ has also been known for a long time [14, 15, 16]. However, until recently a complete understanding of global structure of this solutions was missing. It was elucidated in series of papers [17, 18, 19] in the case $\Lambda > 0$, and in Refs. [20, 21, 22] for $\Lambda < 0$ (cf. also Refs. [23, 24, 25, 26] for related work and discussion of special and degenerated cases).

The C-metric is one of few explicitly known spacetimes representing the gravitational field of nontrivially moving sources. Therefore, it is interesting, for example, as a test-bed for numerical simulations. It plays also an important role in a study of radiative properties of gravitational fields. Namely, in the case of nonvanishing cosmological constant it may provide us with an insight into the character of radiation, which in the asymptotically nontrivial spacetimes is not yet well understood. In Refs. [19, 22] the C-metric spacetimes with $\Lambda \neq 0$ were used to investigate the directional structure of radiation. These results were later generalized [27, 28] for general spacetimes with spacelike and timelike conformal infinity. The C-metric spacetimes have found also successful application to the problem of cosmological pair creation of black holes [29, 30, 31, 32, 33, 34]. In addition to spacetime with accelerated black holes, the C-metric can also describe accelerated naked singularities or, for special choice of parameters, empty spacetime described in a coordinate system adapted to accelerated observers [17, 35, 36].

In the present work we wish to give a complete description of the case when the C-metric describes black holes moving with an acceleration in anti-de Sitter universe. As was already observed in [21, 22, 26], there are three qualitatively different cases according to value of the black hole acceleration A. For small values of acceleration, $A < 1/\ell$, (ℓ being a length scale given by the cosmological constant, cf. Eq. (2.3)) the C-metric describes one accelerated black hole in asymptotically anti-de Sitter spacetime. For large acceleration, $A > 1/\ell$, it describes a sequence of pairs of black holes. In the critical case $A = 1/\ell$ it describes a sequence of single accelerated black holes entering and leaving asymptotically anti-de Sitter spacetime. Here we concentrate on the generic situation $A \neq 1/\ell$; the critical case will be discussed separately [37] (cf. also Refs. [24, 25]).

The main goal of the work is to give a clear visual representation of the global structure of the spacetimes. It is achieved with help of a number of two-dimensional and three-dimensional diagrams. Also, the relation to an empty anti-de Sitter universe is explored. Understanding of the anti-de Sitter spacetime in accelerated coordinates plays a key role in the construction of three-dimensional diagrams for the full C-metric spacetime.

The paper is organized as follows. In Sec. II we overview the C-metric solution with a negative cosmological constant in various coordinate systems. Namely, we introduce coordinates $\tau, \upsilon, \xi, \varphi$, closely related to those of [5] and [14], accelerated static coordinates T, R, Θ, Φ, very useful for physical interpretation, and global null coordinates u, v essential for a study of the global structure. In Secs. III and IV we discuss the two qualitatively different cases of small and large acceleration, respectively. Finally, Sec. V studies the weak field limit, i.e.,

*Electronic address: Pavel.Krtous@mff.cuni.cz

the limit of vanishing mass and charge. In this case the C-metric describes empty-anti de-Sitter universe in accelerated coordinates. The relation of these coordinates to the standard cosmological coordinates is presented, again separately for $A \lessgtr 1/\ell$.

Even more elaborated visual presentation of the studied spacetimes, including animations and interactive three-dimensional diagrams, can be found in [38]. Let us also note that the on-line version of this work includes figures in color.

II. THE C-METRIC WITH A NEGATIVE COSMOLOGICAL CONSTANT

The C-metric with a cosmological constant $\Lambda < 0$ can be written as

$$\boldsymbol{g} = \frac{1}{A^2(x+y)^2}\Big(-F\,\mathbf{d}t^2 + \frac{1}{F}\,\mathbf{d}y^2 + \frac{1}{G}\,\mathbf{d}x^2 + G\,\mathbf{d}\varphi^2\Big)\;, \tag{2.1}$$

where F and G are polynomially dependent on y and x respectively,

$$\begin{aligned} F &= \frac{1}{A^2\ell^2} - 1 + y^2 - 2mA\,y^3 + e^2A^2\,y^4\;,\\ G &= \qquad\;\; 1 - x^2 - 2mA\,x^3 - e^2A^2\,x^4\;. \end{aligned} \tag{2.2}$$

Here ℓ is a length scale given by the cosmological constant Λ,

$$\ell = \sqrt{-\frac{3}{\Lambda}}\;. \tag{2.3}$$

The metric is a solution of the Einstein-Maxwell equations with the electromagnetic field given by

$$\boldsymbol{F} = e\,\mathbf{d}y \wedge \mathbf{d}t\;. \tag{2.4}$$

Depending on the choice of parameters and of ranges of coordinates, the metric (2.1) can describe different spacetimes. In the physically most interesting cases, it describes black holes uniformly accelerated in anti-de Sitter universe. In these cases the constants A, m, e, and C (such that $\varphi \in (-\pi C, \pi C)$) characterize the acceleration, mass and charge of the black holes, and the conicity of the φ symmetry axis, respectively. These parameters have to satisfy $m \geq 0$, $e^2 < m^2$, A, $C > 0$, and the function G must be vanishing for four different values of x in the charged case (e, $m \neq 0$), or for three different values in the uncharged case ($e = 0$, $m \neq 0$). The coordinate x must belong to an interval around zero on which G is positive, and $y \in (-x, \infty)$, cf. Figs. 1 and 5. It follows that $0 \leq G \leq 1$. The boundary values of the allowed range of the coordinate x correspond to different parts of the axis of φ symmetry separated from each other by black holes.

The spacetime described by the C-metric is static and axially-symmetric with Killing vectors $\boldsymbol{\partial}_t$ and $\boldsymbol{\partial}_\varphi$, respectively. Killing horizons of the vector $\boldsymbol{\partial}_t$ are given by condition $F = 0$. They coincide with horizons of various kinds as will be described below. Beside the Killing vectors, the geometry of spacetime possesses one conformal Killing tensor $\boldsymbol{Q}$,

$$\boldsymbol{Q} = \frac{1}{A^4(x+y)^4}\Big(F\,\mathbf{d}t^2 - \frac{1}{F}\,\mathbf{d}y^2 + \frac{1}{G}\,\mathbf{d}x^2 + G\,\mathbf{d}\varphi^2\Big)\;. \tag{2.5}$$

There exist two doubly-degenerate principal null directions

$$\boldsymbol{k}_1 \propto \boldsymbol{\partial}_t - F\boldsymbol{\partial}_y\;,\quad \boldsymbol{k}_2 \propto \boldsymbol{\partial}_t + F\boldsymbol{\partial}_y\;, \tag{2.6}$$

so that the spacetime is of the Petrov type D. The metric has a curvature singularity for $y \to \pm\infty$.

The constants m and e parametrize the mass and charge of black holes. Let us emphasize that they are not directly the mass or charge defined through some invariant integral procedure. For example, the total charge defined by integration of the electric field over a surface around one black hole is $Q = \frac{1}{2}\Delta x C e$. It is proportional to e, but besides the trivial dependence on the conicity C, it depends also on the mass and the acceleration parameters through the length Δx of the allowed range of the coordinate x.

The parameter C defines a range of the angular coordinate φ, and thus it governs a regularity of the φ symmetry axis. Typically, the axis has a conical singularity which corresponds to a string or strut. By an appropriate choice of C, a part of the axis can be made regular. However, for nonvanishing acceleration it is not possible to achieve regularity of the whole axis—objects on the axis are physically responsible for the 'accelerated motion' of black holes.

The constant A parametrizes the acceleration of the black holes. But it is not a simple task to define what it is the *acceleration* of a black hole. The acceleration of a test particle is defined with respect of a local inertial frame given by a background spacetime. However, black holes are objects which deform the spacetime in which they are moving; they define the notion of inertial observers, and they are actually dragging inertial frames with themselves. Therefore, it is not possible to measure the acceleration of black holes with respect to their surroundings. The motion of black holes can be partially deduced from a structure of the whole spacetime, e.g., from a relation of black holes and asymptotically free observers, and partially by investigating a weak field limit in which the black holes become test particles and cease to deform the spacetime around them. Namely, in the limit of vanishing mass and charge, the spacetime (2.1) reduces to the anti-de Sitter universe with black holes changed into worldlines of uniformly accelerated particles. Such a limit will be discussed in Sec. V.

Depending on the value of the parameter A, the metric (2.1) describes qualitatively different spacetimes. For A smaller then a critical value $1/\ell$ given by the cosmological constant, cf. Eq. (2.3), the metric represents asymptotically anti-de Sitter universe with one uniformly accelerated black hole inside.[1] For $A > 1/\ell$ the metric (2.1) describes asymptotically anti-de Sitter spacetime which contains a sequence of pairs of uniformly accelerated black holes which enter and leave the universe through its conformal infinity.[2] The extremal case $A = 1/\ell$ corresponds to accelerated black holes entering and leaving the anti-de Sitter universe, one at a time. This extreme case will not discussed here; however, see Refs. [24, 25, 37].

Coordinates t, y, x, φ can be rescaled in a various way. We will introduce coordinates $\tau, \upsilon, \xi, \varphi$ and closely related accelerated static coordinates T, R, Θ, Φ which are appropriate for a discussion of the limits of weak field and of vanishing acceleration. They will be used thoroughly in the following sections. We will also mention coordinates $\mathfrak{t}, \mathfrak{y}, \mathfrak{x}, \phi$ (used in Ref. [14]) in which the global prefactor A^{-2} in the metric (2.1) is transformed into metric functions, coordinates $\tau, \omega, \sigma, \varphi$ adapted to the infinity, and global null coordinates u, v, ξ, φ. However, detailed transformations among these coordinates differs for the qualitatively different cases $A \lesseqgtr 1/\ell$. Therefore, we list first only metric forms in these coordinate systems and coordinate transformation which are general, and we postpone specific definitions to the next sections.

The metric (2.1) in the coordinate systems t, y, x, φ, $\tau, \upsilon, \xi, \varphi$ and $\mathfrak{t}, \mathfrak{y}, \mathfrak{x}, \phi$ has actually the same form, only with different metric functions (cf. Eqs. (3.5), (3.7), and (4.5), (4.7))

$$\boldsymbol{g} = \frac{\ell^2}{\omega^2}\left(-\mathcal{F}\,\mathbf{d}\tau^2 + \frac{1}{\mathcal{F}}\,\mathbf{d}\upsilon^2 + \frac{1}{\mathcal{G}}\,\mathbf{d}\xi^2 + \mathcal{G}\,\mathbf{d}\varphi^2\right) . \qquad (2.7)$$

$$\boldsymbol{g} = \frac{\ell^2}{(\mathfrak{x}+\mathfrak{y})^2}\left(-\mathfrak{F}\,\mathbf{d}\mathfrak{t}^2 + \frac{1}{\mathfrak{F}}\,\mathbf{d}\mathfrak{y}^2 + \frac{1}{\mathfrak{G}}\,\mathbf{d}\mathfrak{x}^2 + \mathfrak{G}\,\mathbf{d}\phi^2\right) , \qquad (2.8)$$

Accelerated static coordinates T, R, Θ, Φ are given by

$$\begin{gathered} T = \ell\tau\ , \quad R = \frac{\ell}{\upsilon}\ , \quad \Phi = \varphi\ , \\ \mathbf{d}\Theta = \frac{1}{\sqrt{\mathcal{G}}}\,\mathbf{d}\xi\ , \qquad \Theta = \frac{\pi}{2} \quad \text{for} \quad \xi = 0\ . \end{gathered} \qquad (2.9)$$

The metric takes a form

$$\boldsymbol{g} = \frac{\ell^2}{\omega^2 R^2}\left(-\mathcal{H}\,\mathbf{d}T^2 + \frac{1}{\mathcal{H}}\,\mathbf{d}R^2 + R^2\big(\mathbf{d}\Theta^2 + \mathcal{G}\,\mathbf{d}\Phi^2\big)\right) , \qquad (2.10)$$

$$\mathcal{H} = \frac{1}{\upsilon}\mathcal{F}\ ; \qquad (2.11)$$

see (3.9) and (4.8).

The coordinate R is not well-defined at $\upsilon = 0$. It is a coordinate singularity which can be avoided by using the coordinate υ. However, near the black hole, the coordinate R has a more direct physical meaning—it is the radial coordinate measured by area, at least in the conformally related geometry. Because υ can be negative, R can take also negative values. However, it happens only far away from the black holes or in spacetime domains in which R changes into a time coordinate.

The coordinate ξ is given by $\xi = -x$ (cf. Eqs. (3.2) and (4.2)), so we can use what was said about range of definition of x. Let $[\xi_{\mathrm{b}}, \xi_{\mathrm{f}}]$ be the interval of allowed values of ξ, i.e., the interval where $\mathcal{G}$ is positive and $\xi_{\mathrm{b}} < 0 < \xi_{\mathrm{f}}$. The value ξ_{f} corresponds to the axis of φ symmetry (since $\mathcal{G} = 0$ at $\xi = \xi_{\mathrm{f}}$) pointing out of the black hole in the forward direction of the motion.[3] The value ξ_{b} corresponds to the axis (again, $\mathcal{G}|_{\xi=\xi_{\mathrm{b}}} = 0$) going in the opposite (backward) direction. Integrating $1/\sqrt{\mathcal{G}}$ in (2.9), we find that the longitudinal angular coordinate Θ belongs into an interval $[\Theta_{\mathrm{b}}, \Theta_{\mathrm{f}}]$ which, in general, differs from $[0, \pi]$.

If we use the conformal prefactor in the metric (2.7) as a coordinate, and if we find a complementary coordinate σ such that the metric is diagonal (see (3.10) and (4.9)), we get

$$\boldsymbol{g} = \frac{\ell^2}{\omega^2}\left(-\mathcal{F}\,\mathbf{d}\tau^2 + \frac{1}{\mathcal{E}}\left(\mathbf{d}\omega^2 + \mathcal{F}\mathcal{G}\,\mathbf{d}\sigma^2\right) + \mathcal{G}\,\mathbf{d}\varphi^2\right) , \qquad (2.12)$$

This coordinate system is well adapted to the infinity $\mathcal{I}$, since $\mathcal{I}$ is given by $\omega = 0$.

Finally, for discussion of global structure of the spacetime it is useful to introduce global null coordinates[4] u, v, ξ, φ. We start with the 'tortoise' coordinate υ_*

$$\mathbf{d}\upsilon_* = \frac{1}{\mathcal{F}}\,\mathbf{d}\upsilon \qquad (2.13)$$

It expands each of the intervals between successive zeros of $\mathcal{F}$ to the whole real line. Next we define null coordinates $\bar{u}, \bar{v}$

$$\bar{u} = \upsilon_* + \tau\ , \quad \bar{v} = \upsilon_* - \tau\ . \qquad (2.14)$$

These coordinates cover distinct domains of the spacetime which are separated from each other by horizons, i.e., by null surfaces $\mathcal{F} = 0$. The coordinates can be extended across a chosen horizon with help of global coordinates u, v:

$$\begin{aligned} \tan\frac{u}{2} &= (-1)^m \exp\frac{\bar{u}}{2\,|\delta|}\ , \\ \tan\frac{v}{2} &= (-1)^n \exp\frac{\bar{v}}{2\,|\delta|}\ . \end{aligned} \qquad (2.15)$$

---

[1] As for non-accelerated black holes, it is possible to extend the spacetime through interior of the black hole to other asymptotically anti-de Sitter domain(s). However, for $A < 1/\ell$, there is only one black hole in each of these domains.

[2] Again, there can be more asymptotically anti-de Sitter domains, each of them with the described structure.

[3] By the direction of motion we mean the direction from which the black hole is pulled by the cosmic string or toward which it is pushed by the strut. In the weak field limit it is the direction of the acceleration.

[4] Notice the difference between v (v) and υ (upsilon). It should be always clear from the context if we speak about null v or radial υ.

Integers m, n label the domains; see Figs. 2, 6 and 16 below. δ is a real constant. The metric reads[5]

$$\boldsymbol{g} = \frac{\ell^2}{\omega^2}\left(\frac{2\,\delta^2\mathcal{F}}{\sin u \sin v}\,\mathbf{d}u \vee \mathbf{d}v + \frac{1}{\mathcal{G}}\,\mathbf{d}\xi^2 + \mathcal{G}\,\mathbf{d}\varphi^2\right)\,. \tag{2.16}$$

For a suitable choice of the constant δ the metric coefficients turn to be smooth and nondegenerate as functions of coordinates u, v across a chosen horizon. For such a choice we require that the coordinate map u, v, ξ, φ on a neighborhood of that horizon belongs to the differential atlas of the manifold. The metric is thus smoothly extended across the chosen horizon.

III. A SINGLE ACCELERATED BLACK HOLE

A. Coordinate systems

We start a specific discussion with the simpler case

$$A < \frac{1}{\ell}\,. \tag{3.1}$$

The coordinates $\tau, \upsilon, \xi, \varphi$ and $\mathfrak{t}, \mathfrak{y}, \mathfrak{x}, \phi$ are in this case defined by

$$\begin{aligned} \tau &= \cos\chi_\circ\, \mathfrak{t} &&= \cot\chi_\circ\, t\,,\\ \upsilon &= \frac{1}{\cos\chi_\circ}\,\mathfrak{y} &&= \tan\chi_\circ\, y\,,\\ \xi &= -\frac{1}{\sin\chi_\circ}\,\mathfrak{x} &&= -x\,,\\ \varphi &= \sin\chi_\circ\,\phi &&= \varphi\,, \end{aligned} \tag{3.2}$$

where $\chi_\circ \in [0, \frac{\pi}{2})$ is a parameter characterizing the acceleration,

$$A = \frac{1}{\ell}\sin\chi_\circ\,. \tag{3.3}$$

Its geometrical meaning in the weak field limit will be discussed in Sec. V. The metric functions in (2.7) and (2.8) are given by

$$\begin{aligned} \mathcal{F} &= 1 + \upsilon^2 - 2\,\frac{m}{\ell}\cos\chi_\circ\,\upsilon^3 + \frac{e^2}{\ell^2}\cos^2\chi_\circ\,\upsilon^4\,,\\ \mathcal{G} &= 1 - \xi^2 + 2\,\frac{m}{\ell}\sin\chi_\circ\,\xi^3 - \frac{e^2}{\ell^2}\sin^2\chi_\circ\,\xi^4\,, \end{aligned} \tag{3.4}$$

$$\omega = \upsilon\cos\chi_\circ - \xi\sin\chi_\circ\,, \tag{3.5}$$

and

$$\begin{aligned} \mathfrak{F} &= \cos^2\chi_\circ + \mathfrak{y}^2 - 2\,\frac{m}{\ell}\,\mathfrak{y}^3 + \frac{e^2}{\ell^2}\,\mathfrak{y}^4\,,\\ \mathfrak{G} &= \sin^2\chi_\circ - \mathfrak{x}^2 - 2\,\frac{m}{\ell}\,\mathfrak{x}^3 - \frac{e^2}{\ell^2}\,\mathfrak{x}^4\,. \end{aligned} \tag{3.6}$$

They are related by

$$\begin{aligned} \mathcal{F} &= \cos^{-2}\chi_\circ\,\mathfrak{F} = \tan^2\chi_\circ\,F = 1 - \tfrac{\ell^2}{\cos^2\chi_\circ} S\big(\tfrac{\cos\chi_\circ}{\ell}\upsilon\big)\,,\\ \mathcal{G} &= \sin^{-2}\chi_\circ\,\mathfrak{G} = \qquad\qquad G = 1 + \tfrac{\ell^2}{\sin^2\chi_\circ} S\big(\tfrac{\sin\chi_\circ}{\ell}\,\xi\big)\,, \end{aligned} \tag{3.7}$$

where $S(w)$ is a simple polynomial

$$S(w) = -w^2(1 - 2mw + e^2w^2)\,. \tag{3.8}$$

The functions $\mathcal{H}$ is (cf. Eq. (2.11))

$$\mathcal{H} = 1 + \frac{R^2}{\ell^2} - \cos\chi_\circ\,\frac{2m}{R} + \cos^2\chi_\circ\,\frac{e^2}{R^2}\,. \tag{3.9}$$

The coordinate ω was already defined in Eq. (3.5). The complementary orthogonal coordinate σ can be, in general, given simply only in differential form[6]

$$\begin{aligned} \mathbf{d}\sigma &= \frac{\sin\chi_\circ}{\mathcal{F}}\,\mathbf{d}\upsilon + \frac{\cos\chi_\circ}{\mathcal{G}}\,\mathbf{d}\xi\,,\\ \mathbf{d}\omega &= -\cos\chi_\circ\,\mathbf{d}\upsilon + \sin\chi_\circ\,\mathbf{d}\xi\,. \end{aligned} \tag{3.10}$$

(Here we included also the gradient of ω for completeness.) The metric function $\mathcal{E}$ is given by

$$\mathcal{E} = \mathcal{F}\cos^2\chi_\circ + \mathcal{G}\sin^2\chi_\circ\,. \tag{3.11}$$

At infinity, $\omega = 0$ and $\mathcal{E} = 1$.

B. Global structure

Now we are prepared to discuss the global structure of the spacetime in more details. We start inspecting the metric in the accelerated static coordinates (2.10) with $\mathcal{H}$ given by (3.9). It has a familiar form—if we ignore prefactor $\ell^2/(\omega R)^2$ we get the metric of a nonaccelerated black hole in anti-de Sitter universe in standard static coordinates—except for a different range of Θ and except for $\mathcal{G}$ instead of $\sin^2\Theta$ in front of the $\mathbf{d}\Phi^2$ term. Fortunately, $\sqrt{\mathcal{G}}$ on the allowed range of Θ resembles $\sin\Theta$, and the difference does not affect qualitative properties of the geometry.[7] The conformal prefactor $\ell^2/(\omega R)^2$ does not change the causal structure of the black hole. It justifies our claim that the spacetime contains a black hole. It also gives the interpretation for the coordinates—the accelerated static coordinates are centered around the hole, with R being a radial coordinate, and Θ and Φ longitudinal and latitudinal angular coordinates. T is a time coordinate of external observers staying at a constant distance above the horizon of the black hole. The coordinates $\tau, \upsilon, \xi, \varphi$ are only a different parametrization of the time, radial and angular directions.

[5] $\mathbf{d}u \vee \mathbf{d}v = \mathbf{d}u\,\mathbf{d}v + \mathbf{d}v\,\mathbf{d}u$ is a symmetric tensor product, which is usually loosely written as $2\mathbf{d}u\mathbf{d}v$.

[6] The relations are integrable sice $\mathcal{F}$ depends only on υ and $\mathcal{G}$ on ξ.

[7] Let us mention that for $A = 0$, i.e., for $\chi_\circ = 0$, the metric (2.10) becomes exactly the Reissner-Nordström–anti-de Sitter solution with $\xi = -\cos\Theta$, $\mathcal{G} = \sin^2\Theta$, and $\mathcal{H} = 1 + \frac{R^2}{\ell^2} - \frac{2m}{R} + \frac{e^2}{R^2}$.

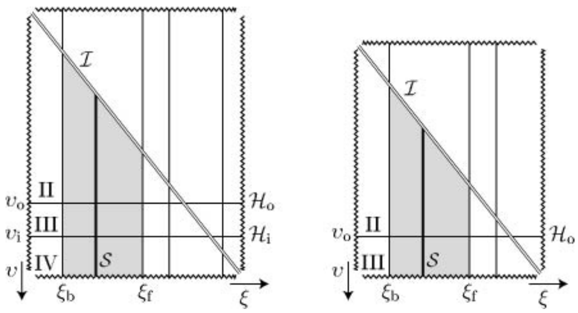

(a) (b)

Figure 1: The diagrams of the allowed range of coordinates v and ξ (the shaded region) in the case of small acceleration $A < 1/\ell$. Diagram (a) is applicable in the charged case, (b) is valid for $m \neq 0$, $e = 0$. ξ_b and ξ_f are zeros of the metric function $\mathcal{G}$ closest to $\xi = 0$. These values correspond to the axis of φ symmetry. The diagonal double-line represents the infinity, cf. Eq. (3.12). The bottom zig-zag line is the singularity at $v = \infty$. v_o and v_i are zeros of the metric function $\mathcal{F}$. They define the outer and inner black hole horizons. They separate the allowed range of coordinates into regions II, III, and IV. These regions corresponds to different domains in spacetime, each of them covered by its own coordinates τ, v, ξ, φ. These coordinate systems cannot be smoothly extended over the horizon. Coordinates smooth across the horizon are used in Fig. 2, where sections $\xi =$ constant are depicted. Such a section is represented in the diagrams above by the vertical thick line.

However, the prefactor $\ell^2/(\omega R)^2$ in (2.10) changes the 'position' of the infinity—the conformal infinity $\mathcal{I}$ is localized at $\omega = 0$, i.e., at

$$v = \tan \chi_o \, \xi \; . \tag{3.12}$$

It means that the radial position of the infinity depends on the direction ξ. This corresponds to the fact that the black hole is not in a symmetrical position with respect to the asymptotically anti-de Sitter universe. Nevertheless, it is in equilibrium—the cosmological compression of anti-de Sitter spacetime (which would push a test body toward any chosen center of the universe) is compensated by a string (or strut) on the axis which keeps the black hole in a static nonsymmetric position with respect to the infinity. We can thus say that the black hole is moving with uniform acceleration equal to the cosmological compression, despite the fact that it cannot be measured locally. Remember that in anti-de Sitter universe a static observer which stays at a fixed spatial position in the spacetime eternally feels the cosmological deceleration of a constant magnitude from the range $[0, 1/\ell)$, depending on his position. This corresponds to the assumption (3.1). As we will see in a moment, we are dealing with *one* black hole which stays *eternally* in equilibrium in asymptotically anti-de Sitter spacetime.

We already said that zeros of $\mathcal{F}$ correspond to Killing horizons of the Killing vector $\boldsymbol{\partial}_\tau$. Inspecting properties of the polynomial $S(w)$, we find that $\mathcal{F} = 0$ for two values $v = v_o, v_i$ $(v_o < v_i)$ in the charged case $(e, m \neq 0)$, and

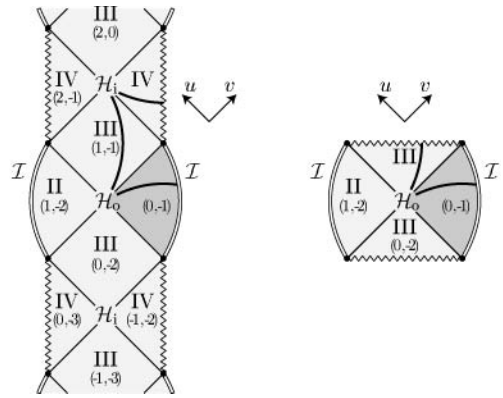

(a) (b)

Figure 2: The conformal diagrams of the sections $\xi, \varphi =$ constant for (a) charged and (b) uncharged C-metric with the acceleration $A < 1/\ell$. These diagrams are based on null coordinates u, v which grow in diagonal directions. Integers (m, n) in the diagrams, identifying different spacetime domains, are those from definition (2.15). Double-lines represent conformal infinity $\mathcal{I}$ (cf. Eq. (3.12)), zig-zag lines the singularity at $v = +\infty$, and thin diagonal lines the outer and inner black hole horizons $v = v_o$ and $v = v_i$, respectively. We can recognize familiar structure of the interior of Reissner-Nordström or Schwarzschild black holes, respectively (domains III and IV). The exterior of the black holes is, however, asymptotically different—it has the asymptotics of anti-de Sitter universe. The whole spacetime consists of more exterior domains II which are connected (not necessary causally) with each other through the black holes. A more detailed diagram of a typical domain outside of the black hole (a darker area indicated above) can be found in Fig. 3b. The thick line corresponds to a section $\tau =$ constant which is discussed in Fig. 1.

for just one value $v = v_o$ if $e = 0$, $m \neq 0$. The null surface $v = v_o$ corresponds to the outer black hole horizon, and $v = v_i$ corresponds to the inner black hole horizon.

Allowed ranges of coordinates v, ξ are shown in Fig. 1. Boundary 'zig-zag' lines corresponds to the curvature singularity at $v, \xi \to \pm\infty$. The horizons separate the allowed range into qualitatively different regions II, III, and IV. Region II describes the asymptotically anti-de Sitter domain outside of the black hole, and regions III and IV correspond to the interior of the black hole.

The coordinate systems τ, v, ξ, φ or T, R, Θ, Φ are defined in each of the regions II, III, IV; however, they are singular at the horizons. To extend the spacetime through the horizons, global null coordinates u, v, ξ, φ can be used. It turns out that the global manifold contains more domains of the type II, III, IV, labeled by integers m, n; see Eq. (2.15). From the domain II outside the outer black hole horizon, the spacetime continues into two domains III inside the black hole. These are connected to other asymptotically anti-de Sitter domains II (behind the Einstein-Rosen bridge through the black hole), and, in the charged case, to domains IV behind inner black hole horizons. Each of these domains is cov-

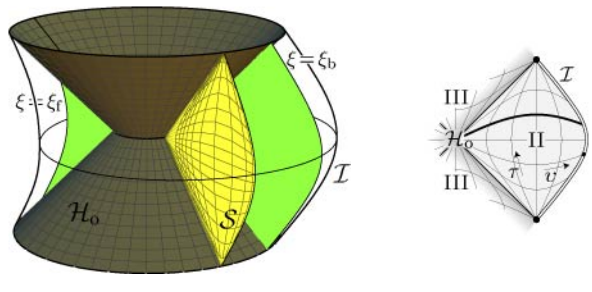

(a) (b)

Figure 3: (a) Three-dimensional representation of the *exterior* of the black hole accelerated in anti-de Sitter universe with acceleration smaller then $1/\ell$. The dark surface represents the outer black hole horizon $\mathcal{H}_o$, and the boundary of the diagram corresponds to the conformal infinity $\mathcal{I}$. Embeddings of a typical section $\xi =$ constant (section $\mathcal{S}$) and of the axis $\xi = \xi_f, \xi_b$ are shown. The nonsymmetric shape of the infinity reflects the fact that the coordinate system used is centered around the black hole which is moving with acceleration with respect to the infinity. (b) Two-dimensional conformal diagram of $\xi =$ constant section. Only the exterior of the black hole is shown (compare with Fig. 2). This part of the conformal diagram corresponds exactly to the section $\xi =$ constant indicated in the diagram on the left.

ered by its own coordinate system $\tau, \upsilon, \xi, \varphi$. This global structure is well illustrated in two-dimensional conformal diagrams of $\xi, \varphi =$ constant sections; see Fig. 2.

As already mentioned, the inner structure of the black hole is qualitatively the same as the structure of the interior of the standard Schwarzschild or Reissner-Nordström black holes. Therefore we focus mainly on the exterior of the black hole. A more detailed conformal diagram of the domain outside of the outer horizon can be found in Fig. 3b. The position of the infinity in the diagrams for various values of ξ changes according to (3.12). We can glue sheets of different ξ together into three-dimensional diagram in Fig. 3a, where only the coordinate φ is suppressed. The 'gluing' is done using an intuition that ξ is a 'deformed cosine' of longitudinal angle and that υ parametrizes the radial direction. The three-dimensional diagram in Fig. 3a is thus obtained by a rotation of the conformal diagram in Fig. 3b.

The outer black hole horizon has a form of two cone-like surfaces joined in the neck of the black hole. The conical shape suggests that horizon is a null surface with null generators originating from the neck. Of course, the three-dimensional diagram does not have the nice feature of the two-dimensional conformal diagrams that each line with angle $\pi/4$ from the vertical is null; however, for Fig. 3a this feature still holds for lines in radial planes, i.e., it holds for generators of the black hole horizon.

In the weak field limit the black hole changes into a test particle. For such a transformation the diagram in Fig. 3a is not very intuitive—the black hole is represented there as an 'extended' object, and the qualitative shape of the horizon does not change with varying mass and

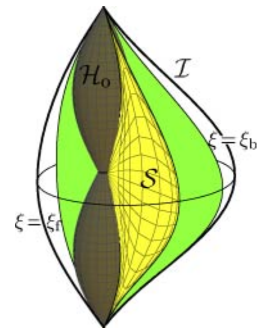

Figure 4: Another three-dimensional representation of the exterior of the accelerated black hole with $A < 1/\ell$. The outer black hole horizon of a conical shape from Fig. 3a is here deformed to the surface of a shape of two joined drops. The black hole is thus represented as a localized object. Such a representation is useful for a study of the weak field limit when the black hole changes into the worldline of a point particle.

charge. For this reason it is useful to draw another diagram in which the black hole horizon is deformed into a shape composed of two drop-like surfaces, see Fig. 4. The conical form of the horizon from Fig. 3a is 'squeezed' into more localized form, which in the limit of vanishing mass and charge shrinks into a worldline of the particle—cf. Fig. 13b in Sec. V.

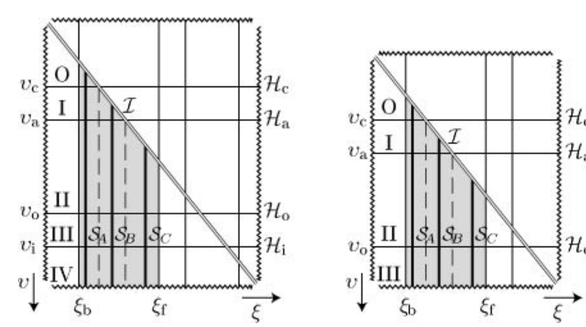

(a) (b)

Figure 5: Diagrams analogous to Fig. 1 in the case $A > 1/\ell$. The allowed range of coordinates υ, ξ (shaded area) is again restricted by the infinity (diagonal double-line), by the axis (vertical border lines), and by the singularity (zig-zag line). Additionally to outer and inner black hole horizons, acceleration and cosmological horizons (at $\upsilon = \upsilon_a$ and $\upsilon = \upsilon_c$) are also present. Horizons divide the allowed range into regions O-IV which corresponds to qualitatively different domains of spacetime; cf. Fig. 6. Different sections $\xi =$ constant cross different number of horizons. Typical representives $\mathcal{S}_A$, $\mathcal{S}_B$, and $\mathcal{S}_C$ of these sections are indicated by thick vertical lines. They correspond to different shapes of the conformal diagrams in Fig. 6.

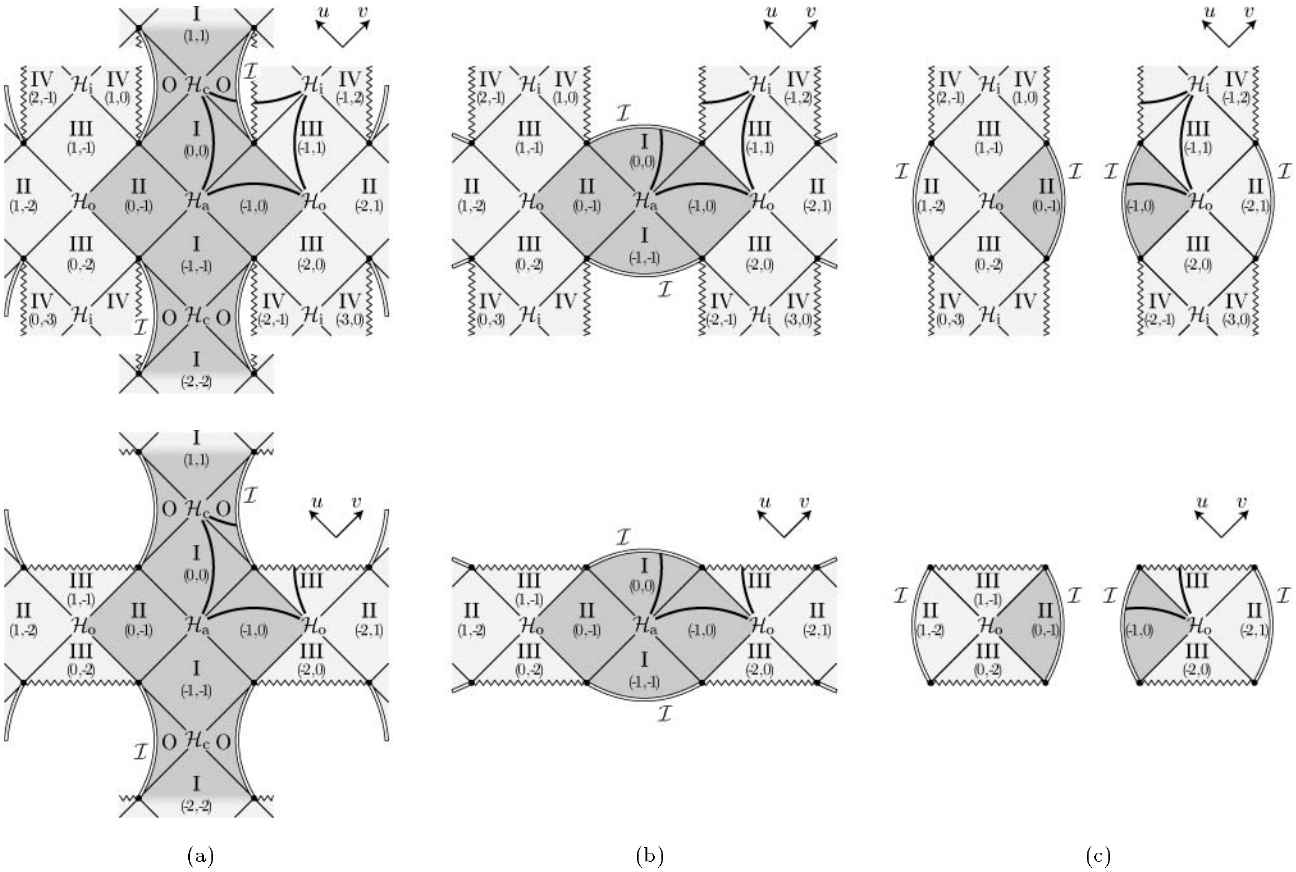

Figure 6: The conformal diagrams of the sections $\xi, \varphi = \text{constant}$ for $A > 1/\ell$. The top diagrams are valid for $m, e \neq 0$, the bottom ones are for the uncharged case. The diagrams are based on coordinates u, v. Integers (m, n) from definition (2.15) identify different domains of the spacetime. Analogously to Fig. 2, double lines represent the infinity, zig-zag lines the singularity, and diagonal lines the horizons. Domains O-II correspond to the exterior of black holes and domains III and IV to interiors of black holes. The interior has a similar causal structure to that of unaccelerated black holes. The spacetime contains more asymptotic domains, one of which is indicated by dark shading. The description below is from a point of view of this domain. Three different shapes of the diagrams correspond to the sections with different value of the coordinate ξ. On the left, section $\mathcal{S}_A$ is spanned between two black holes which are moving with respect to each other along a common axis. It is also spanned between different pairs of such black holes through the domains O and I. In the middle, section $\mathcal{S}_B$ is spanned only between two black holes. It does not continue to other pair of black hole because it intersects the conformal infinity in spacelike lines located inside domains I. The section $\mathcal{S}_C$, depicted on the right, goes from each black hole directly into infinity—it does not connect different black holes through the exterior domains. These three sections correspond to thick vertical lines in Fig. 5. Thick lines in the diagrams above represent the section $\tau = \text{constant}$, i.e., exactly the section discussed in Fig. 5. The embedding of these two-dimensional diagrams into spacetime is shown in Figs. 8–10. More detailed two-dimensional diagrams of the exterior of black holes (the dark area above) are also presented there.

IV. PAIRS OF ACCELERATED BLACK HOLES

A. Coordinate systems

Next we turn to the discussion of the more intricate case of the acceleration bigger than the critical one,

$$A > 1/\ell\,. \tag{4.1}$$

First, the coordinates $\mathfrak{t}, \mathfrak{y}, \mathfrak{x}, \phi$ and $\tau, \xi, \upsilon, \varphi$ can be defined in an analogous way as in the previous section:

$$\begin{aligned}
\tau &= \operatorname{sh}\alpha_{\rm o}\,\mathfrak{t} &&= \tanh\alpha_{\rm o}\;t\,,\\
\upsilon &= \frac{1}{\operatorname{sh}\alpha_{\rm o}}\,\mathfrak{y} &&= \coth\alpha_{\rm o}\;y\,,\\
\xi &= -\frac{1}{\operatorname{ch}\alpha_{\rm o}}\,\mathfrak{x} &&= -x\,,\\
\varphi &= \operatorname{ch}\alpha_{\rm o}\,\phi &&= \varphi\,.
\end{aligned} \tag{4.2}$$

Ranges of the coordinates υ, ξ are indicated in Fig. 5. The acceleration is parametrized by the parameter $\alpha_{\rm o} \in \mathbb{R}^+$,

$$A = \frac{1}{\ell}\cosh\alpha_{\rm o}\,. \tag{4.3}$$

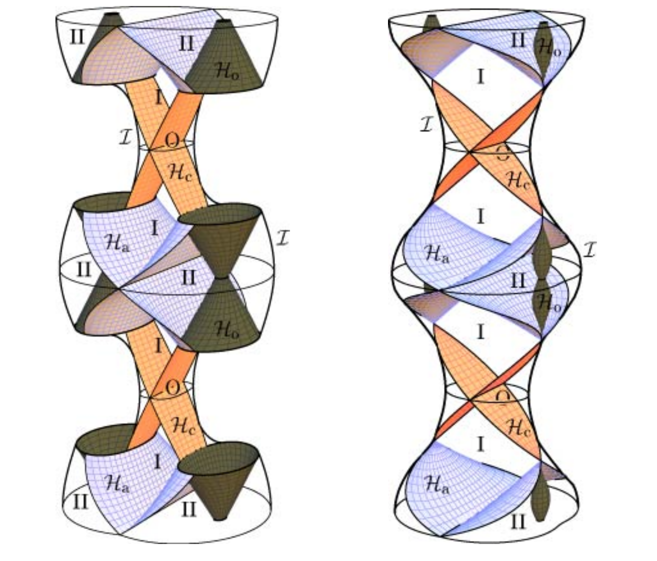

(a) (b)

Figure 7: Three-dimensional visualizations of the *exterior* of black holes which are moving with acceleration parameter $A > 1/\ell$ in asymptotically anti-de Sitter universe. The diagrams show a compactified picture of the whole universe—borders of the diagrams correspond to the conformal infinity. Diagram (a) is obtained by gluing together two-dimensional diagrams from Fig. 6. Black hole outer horizons $\mathcal{H}_{\mathrm{o}}$ are represented by dark surfaces of a conical shape which indicates the null character of these surfaces. In the alternative representation (b), the black hole outer horizons are squeezed into drop-like shapes. Such a representation shows the black hole as a localized object and it is useful in the weak field limit when the black hole changes to a point-like particle—compare with Fig. 17b. The universe represents a sequence of pairs of black holes which repeatedly enter and leave the universe through its timelike infinity—the diagrams should continue periodically in the vertical direction. Black holes of each pair are causally separated by the acceleration horizon $\mathcal{H}_{\mathrm{a}}$; consequent pairs of black holes are separated by cosmological horizons $\mathcal{H}_{\mathrm{c}}$. These are null surfaces—light cones of the 'entry points' of black holes into the spacetime. Embedding of different types of two-dimensional conformal diagrams into the three-dimensional one is depicted in Figs. 8–10.

The metric functions in (2.7) and (2.8) are

$$-\mathcal{F} = 1 - \upsilon^2 + 2\,\frac{m}{\ell}\,\mathrm{sh}\,\alpha_{\mathrm{o}}\,\upsilon^3 - \frac{e^2}{\ell^2}\,\mathrm{sh}^2\,\alpha_{\mathrm{o}}\,\upsilon^4\;,$$
$$\mathcal{G} = 1 - \xi^2 + 2\,\frac{m}{\ell}\,\mathrm{ch}\,\alpha_{\mathrm{o}}\,\xi^3 - \frac{e^2}{\ell^2}\,\mathrm{ch}^2\,\alpha_{\mathrm{o}}\,\xi^4\;, \tag{4.4}$$

$$\omega = \upsilon\;\mathrm{sh}\,\alpha_{\mathrm{o}} - \xi\;\mathrm{ch}\,\alpha_{\mathrm{o}}\;, \tag{4.5}$$

and

$$-\mathfrak{F} = \mathrm{sh}^2\,\alpha_{\mathrm{o}} - \mathfrak{y}^2 + 2\,\frac{m}{\ell}\,\mathfrak{y}^3 - \frac{e^2}{\ell^2}\,\mathfrak{y}^4\;,$$
$$\mathfrak{G} = \mathrm{ch}^2\,\alpha_{\mathrm{o}} - \mathfrak{x}^2 + 2\,\frac{m}{\ell}\,\mathfrak{x}^3 - \frac{e^2}{\ell^2}\,\mathfrak{x}^4\;. \tag{4.6}$$

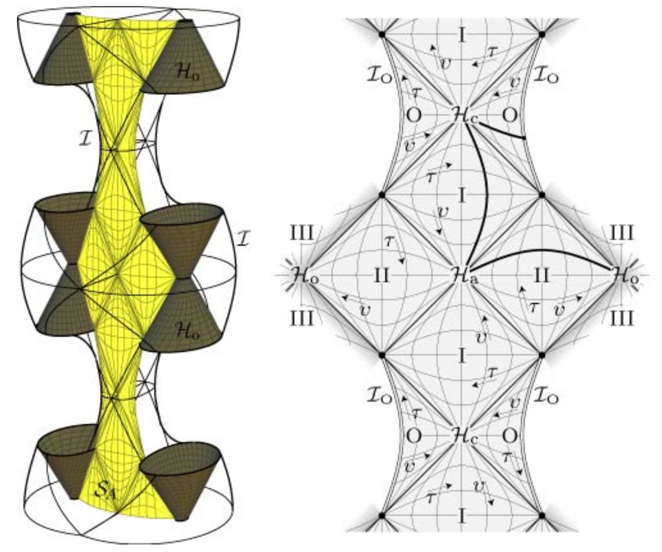

(a) (b)

Figure 8: (a) Embedding of section $\mathcal{S}_A$ (cf. Figs. 5 and 6a) into a three-dimensional representation of the C-metric spacetime. (b) The part of the two-dimensional conformal diagram of $\mathcal{S}_A$ representing the exterior of the black holes (corresponds to the dark area in Fig. 6a).

They are again related to the polynomial (3.8)

$$\begin{aligned} -\mathcal{F} &= -\,\mathrm{sh}^{-2}\chi_{\mathrm{o}}\;\mathfrak{F} = -\coth^2\chi_{\mathrm{o}}\;F = 1 + \tfrac{\ell^2}{\mathrm{sh}^2\alpha_{\mathrm{o}}} S\big(\tfrac{\mathrm{sh}\,\alpha_{\mathrm{o}}}{\ell}\upsilon\big)\;,\\ \mathcal{G} &= \quad \mathrm{ch}^{-2}\alpha_{\mathrm{o}}\;\mathfrak{G} = \qquad\qquad G = 1 + \tfrac{\ell^2}{\mathrm{ch}^2\alpha_{\mathrm{o}}} S\big(\tfrac{\mathrm{ch}\,\alpha_{\mathrm{o}}}{\ell}\,\xi\big)\;. \end{aligned} \tag{4.7}$$

For the metric function $\mathcal{H}$, given by Eq. (2.11), we obtain

$$\mathcal{H} = 1 - \frac{R^2}{\ell^2} - \mathrm{sh}\,\alpha_{\mathrm{o}}\,\frac{2m}{R} + \mathrm{sh}^2\,\alpha_{\mathrm{o}}\,\frac{e^2}{R^2}\;. \tag{4.8}$$

Differential relations for the coordinates σ and ω are

$$\begin{aligned} \mathbf{d}\sigma &= \frac{\mathrm{ch}\,\alpha_{\mathrm{o}}}{\mathcal{F}}\,\mathbf{d}\upsilon + \frac{\mathrm{sh}\,\alpha_{\mathrm{o}}}{\mathcal{G}}\,\mathbf{d}\xi\;,\\ \mathbf{d}\omega &= -\,\mathrm{sh}\,\alpha_{\mathrm{o}}\,\mathbf{d}\upsilon + \mathrm{ch}\,\alpha_{\mathrm{o}}\,\mathbf{d}\xi\;, \end{aligned} \tag{4.9}$$

and the metric function $\mathcal{E}$ takes the form

$$\mathcal{E} = \mathcal{F}\,\mathrm{sh}^2\,\alpha_{\mathrm{o}} + \mathcal{G}\,\mathrm{ch}^2\,\alpha_{\mathrm{o}}\;. \tag{4.10}$$

B. Global structure

As in the previous case, we start with a discussion of the metric in accelerated static coordinates, Eq. (2.10). Near the outer and inner horizon (the smallest two zeros of $\mathcal{H}$), the metric function (4.8) has a similar behavior as the function (3.9). It means that we deal again with a black hole, and near (or inside of) the black hole we can apply the previous discussion. Namely, T is again a time coordinate for observers staying outside black hole, R is

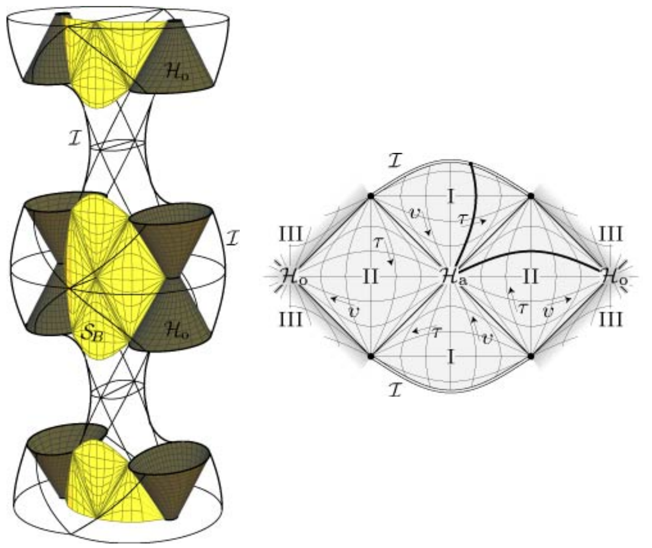

(a) (b)

Figure 9: (a) Embedding of section $\mathcal{S}_B$ (cf. Figs. 5 and 6b) into a three-dimensional picture of spacetime. (b) The corresponding part of the two-dimensional conformal diagram of $\mathcal{S}_B$ (cf. the dark area in Fig. 6b).

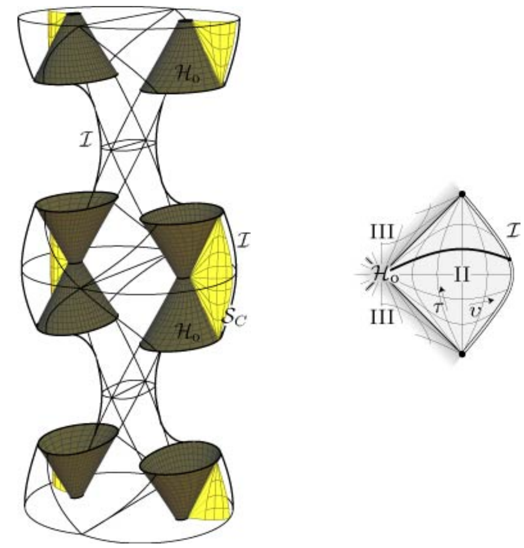

(a) (b)

Figure 10: (a) Embedding of section $\mathcal{S}_C$ (cf. Figs. 5 and 6c) into a three-dimensional diagram. (b) The corresponding part of the two-dimensional conformal diagram of $\mathcal{S}_C$ (cf. the dark areas in Fig. 6c).

a radial coordinate, and Θ, Φ are spherical-like angular coordinates. Similar interpretation hold for the coordinates $\tau, \upsilon, \xi, \varphi$. However, for $A > 1/\ell$ the metric function $\mathcal{H}$ (or, equivalently, $\mathcal{F}$, cf. Eq. (2.11)) has two additional zeros for $R = R_{\rm a}, R_{\rm c}$ ($\upsilon = \upsilon_{\rm a}, \upsilon_{\rm c}$, respectively), which correspond to acceleration and cosmological horizons. It means that we have to expect a more complicated structure of spacetime outside the black hole.

Indeed, from the ξ-υ diagram in Fig. 5 we see that new zeros divide the allowed range of coordinates into more regions O, I, II, III, and IV. An exact way how these domains can be reached through the horizons can be seen from the conformal diagrams of the sections $\xi, \varphi = $ constant. However, in Fig. 5 we see that sections $\xi, \varphi = $ constant can cross different number of horizons, depending on the value of ξ, since they can reach the infinity, given in this case by

$$\upsilon = \coth \alpha_{\rm o}\, \xi \;, \tag{4.11}$$

before they cross the acceleration or cosmological horizons. There are three different generic classes of sections $\xi, \varphi = $ constant labeled $\mathcal{S}_A$ (sections crossing all horizons), $\mathcal{S}_B$ (sections which do not cross cosmological horizons), and $\mathcal{S}_C$ (which cross only black hole horizons). Special limiting cases are $\xi = \xi_{\rm c} = \upsilon_{\rm c} \tanh \alpha_{\rm o}$ and $\xi = \xi_{\rm a} = \upsilon_{\rm a} \tanh \alpha_{\rm o}$. For each of these sections a different shape of conformal diagram is obtained as can be found in Fig. 6. For section $\mathcal{S}_A$ the domain II outside a black hole is connected through the acceleration horizon to domains of type I which are connected through other acceleration horizons to another domain II with another black hole. The domain I is also connected through the cosmological horizon with two domains of type O. From these domains it possible to reach another domain I, and so on.

The spacetime thus seems to describe a universe which at one moment contains a pair of black holes (domains III and IV) separated by the acceleration horizon (domains II and I), and at another moment does not contain any black hole (domains I and O)—see Fig. 6a. However, the sections $\mathcal{S}_B$ do not contain domains O, and sections $\mathcal{S}_C$ do not even contain the domains I. How is it possible that one spacetime is described by three qualitatively different diagrams? And how is it possible that the spacetime with anti-de Sitter asymptotic has a conformal diagram with conformal infinity which looks spacelike as it occurs for sections $\mathcal{S}_B$ (see Fig. 6b)?

The answer can be given by drawing three-dimensional diagram obtained by 'gluing' different sections of $\xi = $ constant together. The inspiration how to do it can be obtained by a study of accelerated static coordinates in empty anti-de Sitter universe as will be done in Sec. V. There we will learn that coordinates $\tau, \upsilon, \xi, \varphi$ (or T, R, Θ, Φ) are sorts of bi-polar coordinates—coordinates with two poles centered on two black holes. The coordinate R (respectively υ) is running through domain II from both black holes toward the acceleration horizon. It plays the role of a radial coordinate in domain II, but it changes its meaning into a time coordinate above and below the acceleration horizon, in domains of type I. It becomes again a space coordinate in domains O. The angular coordinates Θ, Φ (or ξ, φ) label different directions connecting the two holes. With this insight we can draw the three-dimensional diagrams reflecting the global structure of the universe, see Fig. 7. Embeddings of three typical surfaces $\xi, \varphi = $ constant into such a diagram are shown in Figs. 8–10. Here we can see an origin of different shapes of conformal diagrams.

The global picture of the universe is thus the following: into an empty anti-de Sitter-like universe (domains O and I) enters through the infinity $\mathcal{I}$ a pair of black holes (domains III and IV). The holes are flying toward each other (domains II) with deceleration until they stop and fly back to the infinity where they leave the universe. They are causally disconnected by the acceleration horizon. There follows a new phase without black holes (again, the domain I and O) followed by a new phase with a pair of black holes. Different pairs of black holes are separated by cosmological horizons.

Again, for purpose of the weak field limit it is convenient to use a visualization with squeezed black hole horizons in Fig. 7b. In this representation, the infinity has a shape which one would expect for asymptotically anti-de Sitter universe. The deformation of the infinity is related to the fact that we use coordinates centered around the black holes. Indeed, the black holes are drawn along straight lines in the vertical direction. As we will see in the next section, such a deformation of the infinity is obtained even for an empty anti-de Sitter universe if it is represented using accelerated coordinates.

V. ANTI-DE SITTER UNIVERSE IN ACCELERATED COORDINATES

The spacetime (2.1) reduces to the anti-de Sitter universe for $m = 0$, $e = 0$. However, the limiting metric is not the anti-de Sitter metric in standard cosmological coordinates. Instead, it is the anti-de Sitter metric in so-called accelerated coordinates which prefer certain accelerated observers. These observers are remnants of the black holes. Investigating this form of the anti-de Sitter metric is useful for understanding of asymptotical structure of the C-metric universe, and of the nature of the coordinate systems used.

The anti-de Sitter metric can be written in cosmological spherical coordinates $\tilde{t}, \chi, \vartheta, \varphi$ as

$$\boldsymbol{g}_{\mathrm{AdS}} = \frac{\ell^2}{\cos^2\chi}\Big(-\mathbf{d}\tilde{t}^2 + \mathbf{d}\chi^2 + \sin^2\chi\,\big(\mathbf{d}\vartheta^2 + \sin^2\vartheta\,\mathbf{d}\varphi^2\big)\Big)\ . \tag{5.1}$$

They can be also called conformally Einstein because they are the standard coordinates on the conformally related Einstein universe. Another useful set of coordinates are cosmological cylindrical coordinates $\tilde{t}, \zeta, \rho, \varphi$ which redefine coordinates χ and ϑ. Surfaces $\tilde{t}, \rho = \text{constant}$ represent cylinders of constant distance from the axis, and surfaces $\tilde{t}, \zeta = \text{constant}$ are planes orthogonal to the axis. They are related to spherical coordinates by a rotation on the conformally related sphere of the Einstein universe by an angle $\pi/2$:

$$\begin{aligned}\cos\chi &= \cos\zeta\cos\rho\ , &\quad \sin\zeta &= \sin\chi\cos\vartheta\ ,\\ \tan\vartheta &= \cot\zeta\sin\rho\ , &\quad \tan\rho &= \tan\chi\sin\vartheta\ .\end{aligned} \tag{5.2}$$

The metric in the cylindrical coordinates reads

$$\boldsymbol{g}_{\mathrm{AdS}} = \frac{\ell^2}{\cos^2\zeta\cos^2\rho}\Big(-\mathbf{d}\tilde{t}^2 + \mathbf{d}\zeta^2 + \cos^2\zeta\,\big(\mathbf{d}\rho^2 + \sin^2\rho\,\mathbf{d}\varphi^2\big)\Big)\ . \tag{5.3}$$

The anti-de Sitter universe admits four qualitatively different types of Killing vectors representing time translations, boosts, null boosts, and spatial rotations. Orbits of time translations and boosts correspond to worldlines of observers with uniform acceleration. The limit of the C-metric is related exactly to these observers. The cases $A < 1/\ell$ and $A > 1/\ell$ correspond to time translation and boost Killing vectors respectively; the case $A = 1/\ell$ corresponds to a null boost Killing vector.

It is possible to introduce static coordinates associated with the Killing vector that is at least partially timelike. In the case of the time translation Killing vector, both cosmological spherical and cylindrical coordinates play the roles of such coordinates. It is also possible to rescale the radial coordinate χ to obtain metric in 'standard static' form. Namely, defining static coordinates of type I

$$T_{\mathrm{I}} = \ell\,\tilde{t}\ ,\quad R_{\mathrm{I}} = \ell\,\tan\chi\ ,\quad \Theta_{\mathrm{I}} = \vartheta\ ,\quad \Phi_{\mathrm{I}} = \varphi \tag{5.4}$$

we obtain

$$\begin{aligned}\boldsymbol{g}_{\mathrm{AdS}} = -\Big(1 + \frac{R_{\mathrm{I}}^2}{\ell^2}\Big)\mathbf{d}T_{\mathrm{I}}^2 + \Big(1 + \frac{R_{\mathrm{I}}^2}{\ell^2}\Big)^{-1}\mathbf{d}R_{\mathrm{I}}^2\\ + R_{\mathrm{I}}^2\big(\mathbf{d}\Theta_{\mathrm{I}}^2 + \sin^2\Theta_{\mathrm{I}}\,\mathbf{d}\Phi_{\mathrm{I}}^2\big)\ .\end{aligned} \tag{5.5}$$

Static coordinates of type II are associated with the boost Killing vector and can be related to the cosmological cylindrical coordinates

$$\begin{gathered}T_{\mathrm{II}} = \frac{\ell}{2}\log\left|\frac{\sin\tilde{t} - \sin\zeta}{\sin\tilde{t} + \sin\zeta}\right|\ ,\quad R_{\mathrm{II}} = \ell\frac{\cos\zeta}{\cos\tilde{t}}\ ,\\ \Theta_{\mathrm{II}} = \rho\ ,\quad \Phi_{\mathrm{II}} = \varphi\ ,\end{gathered} \tag{5.6}$$

leading to the metric

$$\begin{aligned}\boldsymbol{g}_{\mathrm{AdS}} = \frac{\ell^2}{R_{\mathrm{II}}^2\cos^2\Theta_{\mathrm{II}}}\bigg[-\Big(1 - \frac{R_{\mathrm{II}}^2}{\ell^2}\Big)\mathbf{d}T_{\mathrm{II}}^2\\ + \Big(1 - \frac{R_{\mathrm{II}}^2}{\ell^2}\Big)^{-1}\mathbf{d}R_{\mathrm{II}}^2 + R_{\mathrm{II}}^2\big(\mathbf{d}\Theta_{\mathrm{II}}^2 + \sin^2\Theta_{\mathrm{II}}\,\mathbf{d}\Phi_{\mathrm{II}}^2\big)\bigg]\ .\end{aligned} \tag{5.7}$$

In the case of the full C-metric we do not have to use a different notation for coordinates defined in the case $A < 1/\ell$ and $A > 1/\ell$, because these two cases describe completely different spacetimes, and the coordinates cannot be mixed. However, in the weak field limit both cases describe one spacetime—anti-de Sitter universe—and we have a whole set of coordinate systems, parametrized by acceleration, living on this spacetime. To avoid a confusion, in the next two subsections we add a prime and subscript I (for $A < 1/\ell$) or II (for $A > 1/\ell$) to all coordi-

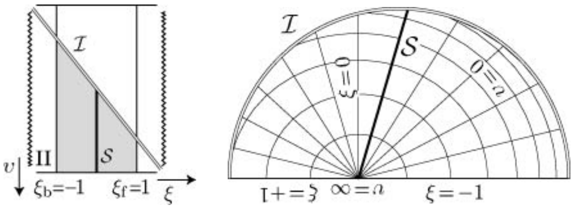

(a) (b)

Figure 11: A shaded region in diagram (a) indicates allowed ranges of coordinates $v \equiv v'_{\rm I} = \ell/R'_{\rm I} = \cot\chi'_{\rm I}$ and $\xi \equiv \xi'_{\rm I} = -\cos\Theta'_{\rm I} = -\cos\vartheta'_{\rm I}$. The diagonal double-line corresponds to the infinity, vertical borders to the axis of symmetry and the bottom line to the origin $\chi'_{\rm I} = 0$. The diagram (a) is an analogue of Fig. 1. However, this diagram does not respect the angular meaning of the ξ coordinate. A more natural representation (b) of the shaded region is obtained by shrinking the bottom line to a point, forming thus a deformed semicircle.

nates introduced in the previous sections.[8] For example, accelerated static coordinates T, R, Θ, Φ will be renamed as $T'_{\rm I}, R'_{\rm I}, \Theta'_{\rm I}, \Phi'_{\rm I}$ or $T'_{\rm II}, R'_{\rm II}, \Theta'_{\rm II}, \Phi'_{\rm II}$ for small or large acceleration, respectively.

Let us note that for both cases $A \lessgtr 1/\ell$ in the weak field limit, the metric function $\mathcal{G}$ reduces to $\mathcal{G} = 1 - \xi^2$ (see (3.4) and (4.4)). By integrating (2.9) we then get $\xi = -\cos\Theta$ and $\mathcal{G} = \sin^2\Theta$.

A. $A < 1/\ell$

In the limit of vanishing mass and charge, the metric (2.10) with $\mathcal{H}$ given by Eq. (3.9) takes the form

$$\boldsymbol{g} = \frac{\ell^2}{\left(\ell\cos\chi_{\rm o} + R'_{\rm I}\sin\chi_{\rm o}\cos\Theta'_{\rm I}\right)^2}\Bigg[-\Big(1+\frac{R'^2_{\rm I}}{\ell^2}\Big)\mathbf{d}T'^2_{\rm I} + \Big(1+\frac{R'^2_{\rm I}}{\ell^2}\Big)^{-1}\mathbf{d}R'^2_{\rm I} + R'^2_{\rm I}\big(\mathbf{d}\Theta'^2_{\rm I} + \sin^2\Theta'_{\rm I}\,\mathbf{d}\Phi'^2_{\rm I}\big)\Bigg]. \tag{5.8}$$

The allowed ranges of coordinates can be read from Fig. 11. For vanishing acceleration, $\chi_{\rm o} = 0$, the metric becomes exactly of the form (5.5); i.e., C-metric accelerated static coordinates become anti-de Sitter static coordinates of type I. For non-vanishing acceleration the form of the metric (5.8) differs from (5.5) by a scalar prefactor. However, we still claim that $\boldsymbol{g} = \boldsymbol{g}_{\rm AdS}$. The relation between coordinates $T_{\rm I}, R_{\rm I}, \Theta_{\rm I}, \Phi_{\rm I}$ and $T'_{\rm I}, R'_{\rm I}, \Theta'_{\rm I}, \Phi'_{\rm I}$

[8] We use the subscript to distinguish two qualitatively different cases (although, we still have a hidden parametrization of the coordinate systems by the acceleration), and the prime to indicate a nontrivial acceleration. Corresponding unprimed coordinates refer to special values of the acceleration: $A = 0$ in the case I, and $A = 1/\ell$ in the case II. This notation is consistent with Ref. [36].

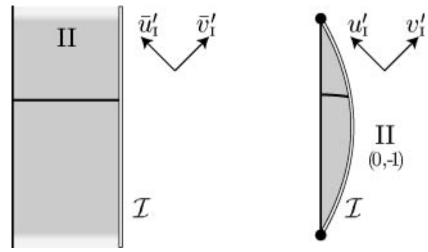

(a) (b)

Figure 12: Conformal diagrams of the section $\Theta'_{\rm I}, \Phi'_{\rm I} = \text{constant}$ (or, equivalently, $\vartheta'_{\rm I}, \varphi'_{\rm I} = \text{constant}$). Diagram (a) is based on coordinates $\bar{u}'_{\rm I}, \bar{v}'_{\rm I}$. Horizontal and vertical lines are given by coordinate lines $\tilde{t}'_{\rm I} = \text{constant}$ and $\chi'_{\rm I} = \text{constant}$, since for $m, e = 0$, definitions (2.13) and (2.14) give $\bar{u}'_{\rm I} = \chi'_{\rm I} + \tilde{t}'_{\rm I}$ and $\bar{v}'_{\rm I} = \chi'_{\rm I} - \tilde{t}'_{\rm I}$. The coordinate $\chi'_{\rm I}$ is a radial coordinate; the left border of the diagram thus corresponds to the worldline of an accelerated observer at the origin. The right double-line represents conformal infinity $\mathcal{I}$ (formed by limiting end points of spacelike and null geodetics). The diagram should continue infinitely in the vertical direction. (b) Compactified version of the same conformal diagram based on the coordinates $u'_{\rm I}, v'_{\rm I}$, related to $\bar{u}'_{\rm I}, \bar{v}'_{\rm I}$ by Eq. (2.15). The whole spacetime is here squeezed into a compact region which beside the conformal infinity includes also point-like future and past infinities (limiting end points of timelike geodesics). This diagram is analogous to those in Fig. 2. An exact position of $\mathcal{I}$ depends on an angular direction of the plane of the diagram (i.e., on a value of coordinate $\vartheta'_{\rm I}$) through the relation $\tan\chi'_{\rm I} = -\ell\cot\chi_{\rm o}/\cos\vartheta'_{\rm I}$ (cf. Eq. (3.12)). For $A = 0$ these diagrams reduces to the standard conformal diagrams based on the cosmological spherical coordinates.

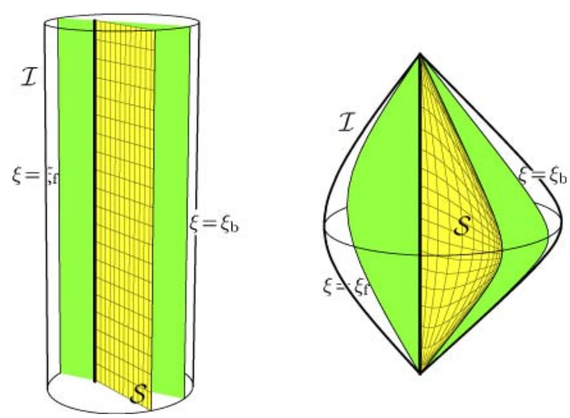

(a) (b)

Figure 13: Three-dimensional schematical diagrams of anti-de Sitter universe obtained by rotation (varying angular coordinate $\vartheta'_{\rm I}$) of two-dimensional diagrams from Fig. 12. The diagrams are centered on the worldline of a static observer (thick line) which is accelerated with acceleration $A < 1/\ell$. The horizontal section $\tilde{t} = \text{constant}$ corresponds to two copies of Fig. 11b (one copy for $\varphi = 0$, another for $\varphi = \pi$).

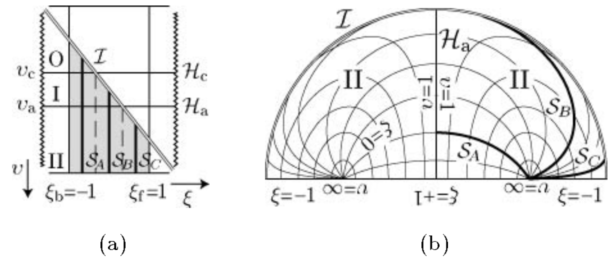

Figure 14: A shaded region in diagram (a) represents the allowed range of coordinates $v \equiv v'_{\text{II}} = \ell/R'_{\text{II}}$ and $\xi \equiv \xi'_{\text{II}} = -\cos\Theta'_{\text{II}}$. The notation is the same as in Fig. 5, except there are no black hole horizons, and the bottom line does not represent a singularity but poles of the coordinates. Diagram (a) does not respect the bi-polar nature of coordinates v and ξ. A more accurate picture of region II is drawn in diagram (b). It depicts section $\tilde{t}, \varphi = 0$ through two spacetime domains of type II. Each of them contains one pole of the coordinate system. Both domains are separated by an acceleration horizon. The coordinate v decreases from $v = +\infty$ at poles to $v = v_a$ at the acceleration horizon, and the coordinate ξ labels different coordinate lines starting from the poles.

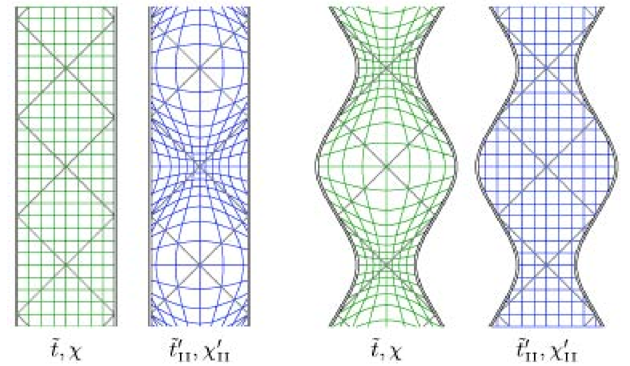

Figure 15: Cosmological spherical coordinates $\tilde{t}, \chi$ and accelerated spherical coordinates $\tilde{t}'_{\text{II}}, \chi'_{\text{II}}$ drawn on a two-dimensional section of anti-de Sitter universe. The coordinate systems are related by the 'squeezing transformation' (5.11). Left: Coordinate lines of both systems drawn in such a way that lines $\tilde{t} = \text{constant}$ and $\chi = \text{constant}$ are horizontal and vertical, respectively. Right: A complementary representation with vertical and horizontal lines given by coordinate system $\tilde{t}'_{\text{II}}, \chi'_{\text{II}}$. The conformal infinity is given by $\chi = \pi/2$ and is thus deformed in the squeezed diagram on the right.

is thus a coordinate conformal transformation of anti-de Sitter space. It has a nice geometrical interpretation: if we define accelerated spherical coordinates of type I, $\tilde{t}'_{\text{I}}, \chi'_{\text{I}}, \vartheta'_{\text{I}}, \varphi'_{\text{I}}$, related to $T'_{\text{I}}, R'_{\text{I}}, \Theta'_{\text{I}}, \Phi'_{\text{I}}$ analogously to definition (5.4), these coordinates differ from $\tilde{t}, \chi, \vartheta, \varphi$ only by a rotation of the Einstein sphere in the direction of the axis $\vartheta = \pi$ by the angle χ_o,

$$\begin{aligned} \tilde{t}'_{\text{I}} &= \tilde{t}\;, \quad \cos\chi'_{\text{I}} = \cos\chi_o \cos\chi - \sin\chi_o \sin\chi \cos\vartheta\;, \\ \varphi'_{\text{I}} &= \varphi\;, \quad \cot\vartheta'_{\text{I}} = \cos\chi_o \cot\vartheta + \sin\chi_o \cot\chi \sin^{-1}\vartheta\;. \end{aligned} \tag{5.9}$$

Coordinates $\tilde{t}'_{\text{I}}, \chi'_{\text{I}}, \vartheta'_{\text{I}}, \varphi'_{\text{I}}$ are thus a sort of spherical coordinates[9] centered on the observer given by $\chi = \chi_o$, $\vartheta = \pi$. This observer remains eternally at a constant distance from the origin $\chi = 0$, and has a unique acceleration of magnitude $A = \sin\chi_o$ which compensates for the cosmological compression of anti-de Sitter universe. For more details see [36].

Two-dimensional conformal diagrams of T'_{I}-R'_{I} sections (i.e., of $\tilde{t}'_{\text{I}}$-χ'_{I} sections) can be found in Fig. 12. Three-dimensional diagrams obtained by gluing together two-dimensional sections with changing Θ'_{I} are in Fig. 13. The diagram in Fig. 13b is clearly the limiting case of Fig. 4.

B. $A > 1/\ell$

In this case, the metric (2.10) with $\mathcal{H}$ given by Eq. (4.8) for vanishing mass and charge becomes

$$\begin{aligned} \boldsymbol{g} = \frac{\ell^2}{\left(\ell\,\mathrm{sh}\,\alpha_o + R'_{\text{II}}\,\mathrm{ch}\,\alpha_o \cos\Theta'_{\text{II}}\right)^2} \bigg[&-\Big(1 - \frac{R'^2_{\text{II}}}{\ell^2}\Big)\mathbf{d}T'^2_{\text{II}} \\ &+ \Big(1 - \frac{R'^2_{\text{II}}}{\ell^2}\Big)^{-1}\mathbf{d}R'^2_{\text{II}} + R^2\big(\mathbf{d}\Theta'^2_{\text{II}} + \sin^2\Theta'_{\text{II}}\,\mathbf{d}\Phi'^2_{\text{II}}\big)\bigg]\;. \end{aligned} \tag{5.10}$$

The allowed range of coordinates $R'_{\text{II}}, \Theta'_{\text{II}}$ can be read from Fig. 14. For $\alpha_o = 0$ (i.e., in the limit $A \to 1/\ell$) we get exactly the metric (5.7). For nonzero α_o both metrics (5.10) and (5.7) have the same form up to a scalar prefactor. However, as in the previous case, it is possible to find a transformation between $T'_{\text{II}}, R'_{\text{II}}, \Theta'_{\text{II}}, \Phi'_{\text{II}}$ and $T_{\text{II}}, R_{\text{II}}, \Theta_{\text{II}}, \Phi_{\text{II}}$ such that $\boldsymbol{g} = \boldsymbol{g}_{\text{AdS}}$. First, we introduce accelerated spherical and cylindrical coordinates of type II, $\tilde{t}'_{\text{II}}, \chi'_{\text{II}}, \vartheta'_{\text{II}}, \varphi'_{\text{II}}$ and $\tilde{t}'_{\text{II}}, \zeta'_{\text{II}}, \rho'_{\text{II}}, \varphi'_{\text{II}}$, which are related to $T'_{\text{II}}, R'_{\text{II}}, \Theta'_{\text{II}}, \Phi'_{\text{II}}$ as $\tilde{t}, \chi, \vartheta, \varphi$ and $\tilde{t}, \zeta, \rho, \varphi$ are related to $T_{\text{II}}, R_{\text{II}}, \Theta_{\text{II}}, \Phi_{\text{II}}$, i.e., by the relations (5.2) and (5.6). Transformations between cosmological and accelerated coordinates then are

$$\begin{aligned} \cot\tilde{t}'_{\text{II}} &= \frac{\mathrm{ch}\,\alpha_o \cos\tilde{t} - \mathrm{sh}\,\alpha_o \cos\chi}{\sin\tilde{t}}\;, \\ \cot\chi'_{\text{II}} &= \frac{-\,\mathrm{sh}\,\alpha_o \cos\tilde{t} + \mathrm{ch}\,\alpha_o \cos\chi}{\sin\chi}\;, \\ \vartheta'_{\text{II}} &= \vartheta\;, \quad \varphi'_{\text{II}} = \varphi\;. \end{aligned} \tag{5.11}$$

It is interesting, that these transformations leave angular coordinates untouched. It means that they are a time dependent *radial* 'sqeezing' of anti-de Sitter universe; see Fig. 15.

Surprisingly, if we compose all partial transformations between $T'_{\text{II}}, R'_{\text{II}}, \Theta'_{\text{II}}, \Phi'_{\text{II}}$ and $T_{\text{II}}, R_{\text{II}}, \Theta_{\text{II}}, \Phi_{\text{II}}$ together, the resulting transformation is such that $T'_{\text{II}} = T_{\text{II}}$

[9] They are spherical in the sense of conformally related Einstein universe.

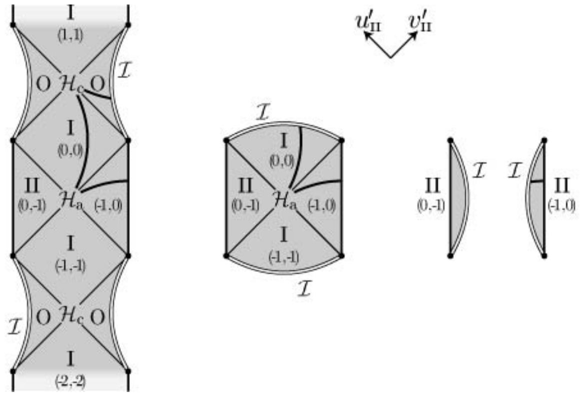

(a) (b) (c)

Figure 16: The conformal diagrams of sections $\xi'_{\rm II}, \varphi'_{\rm II} = \text{constant}$ (or, equivalently, $\rho'_{\rm II}, \varphi'_{\rm II} = \text{constant}$) for different values of $\xi \equiv \xi'_{\rm II}$. The diagrams are based on null coordinates $u'_{\rm II}, v'_{\rm II}$. They are spanned between two poles which corresponds to observers with uniform acceleration $A > 1/\ell$ (straight vertical lines on the border of the diagrams, cf. also Fig. 17 for the three-dimensional localization of the poles). Three different shapes of the diagrams correspond to qualitatively different possibilities of how sections $\xi'_{\rm II}, \varphi'_{\rm II} = \text{constant}$ are embedded into the anti-de Sitter universe. They correspond to the three sections $\xi = \text{constant}$ indicated in Fig. 14. Diagonal lines represent acceleration and cosmological horizons. The acceleration horizon causally separates both poles. It is formed by future light cones of points where the poles enter the anti-de Sitter universe. The cosmological horizon is formed by future light cones of points where the poles leave the universe. The thick line is an example of $v \equiv v'_{\rm II} = \text{constant}$ section—it corresponds to the diagram in Fig. 11. Gluing together diagram (a) for $\xi'_{\rm II} = -1$ (the axis $\rho'_{\rm II} = \Theta'_{\rm II} = 0$ between poles) with diagram (c) for $\xi'_{\rm II} = +1$ (the axis $\rho'_{\rm II} = \Theta'_{\rm II} = \pi$) gives the history of the whole axis of symmetry. It is the same section as that depicted in Fig. 15.

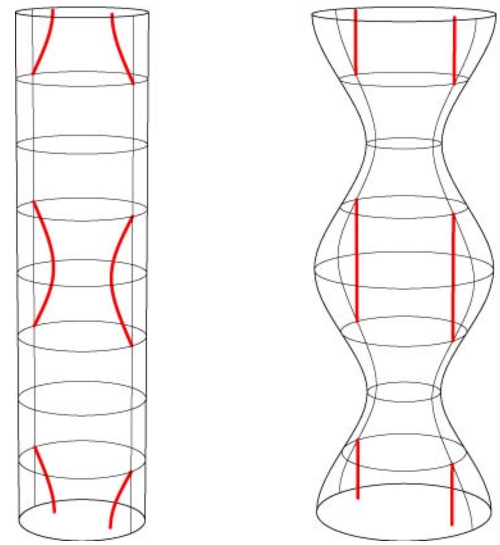

(a) (b)

Figure 17: Three-dimensional representations of anti-de Sitter universe based (a) on cosmological coordinates $\tilde{t}, \chi, \vartheta, \varphi$ and (b) on 'squeezed' accelerated coordinates $\tilde{t}'_{\rm II}, \chi'_{\rm II}, \vartheta'_{\rm II}, \varphi'_{\rm II}$. They can be obtained by a rotation of the corresponding diagrams from Fig. 15. Alternatively, they can be constructed by gluing together two-dimensional diagrams from Fig. 16. These are spanned between worldlines of poles moving with the uniform acceleration $A = 1/\ell$ along the axis. Worldlines of the poles are indicated in the diagrams by thick lines. A pair of the poles enter anti-de Sitter universe through the conformal infinity, they approach each other and then return back to the infinity—all this in a finite cosmological time $\Delta\tilde{t} = \pi$. After a stage without poles, a new pair of poles enters the universe, and so on. The diagram (b) is clearly the limit of Fig. 7b in which the black holes are shrunk to to the accelerated particles located at the poles.

and $\Phi'_{\rm II} = \Phi_{\rm II}$, see Ref. [36]—time surfaces of both the static coordinates of type II and of the accelerated static coordinates are the same.

Now, let us study global null coordinates $u_{\rm II}, v_{\rm II}$ related to the static coordinates of type II $T_{\rm II}, R_{\rm II}$ by the relations (2.14) and (2.15). With vanishing mass and charge (and setting $\delta = 1/2$ in (2.15)) these definitions give

$$\begin{aligned} u_{\rm II} &= \tilde{t} - \zeta\ , \quad \Theta_{\rm II} = \rho\ ,\\ v_{\rm II} &= \tilde{t} + \zeta\ , \quad \Phi_{\rm II} = \varphi \end{aligned} \tag{5.12}$$

Horizontal and vertical lines of the conformal diagram based on $u_{\rm II}, v_{\rm II}$ are thus coordinate lines $\tilde{t} = \text{constant}$ and $\zeta = \text{constant}$. The surface of this conformal diagram, i.e., the surface $\rho, \varphi = \text{constant}$, is a history of a line with a constant distance from the axis of symmetry. All such lines have common limiting end points $\zeta = \pm\pi/2$ located at the infinity of the anti-de Sitter universe. We will call them poles of the cylindrical coordinates.[10]

The conformal diagrams constructed in Sec. IV are based on coordinates $u'_{\rm II}, v'_{\rm II}$, i.e., on an 'accelerated' version of u, v discussed in the previous paragraph. For $m, e = 0$, these diagrams are depicted in Fig. 16. Different sections $\rho'_{\rm II}, \varphi'_{\rm II} = \text{constant}$ again correspond to histories of curves which end at common poles $\zeta'_{\rm II} = \pm\pi/2$. However, the infinity of the anti-de Sitter universe in accelerated cylindrical coordinates is given by (cf. (4.11))

$$\cos\zeta'_{\rm II}\cos\rho'_{\rm II} = -\tanh\alpha_{\rm o}\cos\tilde{t}'_{\rm II}\ . \tag{5.13}$$

[10] Lines of constant distance from the axis are not geodesics (except the axis itself) in sense of the Lobachevsky geometry of the spatial section $\tilde{t} = \text{constant}$. However, in the conformally related spherical geometry of the spatial section of Einstein universe, these lines are meridians with common poles. These two poles lie on the boundary of the hemisphere which corresponds to the Lobachevsky plane, i.e., at its infinity.

The poles thus, in general, do not lie at the infinity. Coordinates $\tilde{t}'_{\text{II}}, \zeta'_{\text{II}}, \rho'_{\text{II}}, \varphi'_{\text{II}}$ are sort of 'bi-polar coordinates' with poles which correspond to the observers with acceleration $A > 1/\ell$; see Fig. 11b. These observers, however, do not remain in anti-de Sitter universe eternally. Their histories periodically enter and leave the spacetime as shown in Fig. 17. The section $\rho'_{\text{II}}, \varphi'_{\text{II}} = \text{constant}$, spanned between the poles, intersect anti-de Sitter universe in various ways, depending on a value of ρ'_{II}. Different intersections lead to qualitatively different conformal diagrams in Fig. 16. This is in the agreement with analogous discussion in Sec. IV.

Acknowledgments

The work was supported in part by program 360/2005 of Ministry of Education, Youth and Sports of Czech Republic. The author is grateful for kind hospitality at the Division of Geometric Analysis and Gravitation, Albert Einstein Institute, Golm, Germany, and the Department of Physics, University of Alberta, Edmonton, Canada where this work was partially done. He also thanks Don N. Page for reading the manuscript.

[1] J. Bičák and B. G. Schmidt, Phys. Rev. D **40**, 1827 (1989).
[2] T. Levi-Civita, Atti Accad. Naz. Lincei, Cl. Sci. Fis., Mat. Nat., Rend. **26**, 307 (1917).
[3] H. Weyl, Ann. Phys. (Leipzig) **59**, 185 (1918).
[4] J. Ehlers and W. Kundt, in *Gravitation: an Introduction to Current Research*, edited by L. Witten (John Wiley, New York, 1962), pp. 49–101.
[5] W. Kinnersley and M. Walker, Phys. Rev. D **2**, 1359 (1970).
[6] A. Ashtekar and T. Dray, Commun. Math. Phys. **79**, 581 (1981).
[7] W. B. Bonnor, Gen. Rel. Grav. **15**, 535 (1983).
[8] J. Bičák and V. Pravda, Phys. Rev. D **60**, 044004 (1999), gr-qc/9902075.
[9] P. S. Letelier and S. R. Oliveira, Phys. Rev. D **64**, 064005 (2001), gr-qc/9809089.
[10] V. Pravda and A. Pravdová, Czech. J. Phys. **50**, 333 (2000), gr-qc/0003067.
[11] K. Hong and E. Teo, Class. Quantum Grav. **20**, 3269 (2003), gr-qc/0305089.
[12] K. Hong and E. Teo, Class. Quantum Grav. **22**, 109 (2005), gr-qc/0410002.
[13] J. B. Griffiths and J. Podolsky, Class. Quantum Grav. **22**, 3467 (2005), gr-qc/0507021.
[14] J. Plebański and M. Demiański, Ann. Phys. (N.Y.) **98**, 98 (1976).
[15] B. Carter, Commun. Math. Phys. **10**, 280 (1968).
[16] R. Debever, Bull. Soc. Math. Belg. **23**, 360 (1971).
[17] J. Podolský and J. B. Griffiths, Phys. Rev. D **63**, 024006 (2001), gr-qc/0010109.
[18] O. J. C. Dias and J. P. S. Lemos, Phys. Rev. D **67**, 084018 (2003), hep-th/0301046.
[19] P. Krtouš and J. Podolský, Phys. Rev. D **68**, 024005 (2003), gr-qc/0301110.
[20] J. Podolský, Czech. J. Phys. **52**, 1 (2002), gr-qc/0202033.
[21] O. J. C. Dias and J. P. S. Lemos, Phys. Rev. D **67**, 064001 (2003), hep-th/0210065.
[22] J. Podolský, M. Ortaggio, and P. Krtouš, Phys. Rev. D **68**, 124004 (2003), gr-qc/0307108.
[23] O. J. C. Dias and J. P. S. Lemos, Phys. Rev. D **68**, 104010 (2003), hep-th/0306194.
[24] R. Emparan, G. T. Horowitz, and R. C. Myers, JHEP **01**, 007 (2000), hep-th/9911043.
[25] A. Chamblin, Class. Quantum Grav. **18**, L17 (2001), hep-th/0011128.
[26] R. Emparan, G. T. Horowitz, and R. C. Myers, JHEP **01**, 021 (2000), hep-th/9912135.
[27] P. Krtouš and J. Podolský, Class. Quantum Grav. **21**, R233 (2004), gr-qc/0502095.
[28] P. Krtouš and J. Podolský, Czech. J. Phys. **55**, 119 (2005), gr-qc/0502096.
[29] R. Emparan, Phys. Rev. Lett. **75**, 3386 (1995), gr-qc/9506025.
[30] R. Emparan, Phys. Rev. D **52**, 6976 (1995), gr-qc/9507002.
[31] R. B. Mann, Class. Quantum Grav. **14**, L109 (1997), gr-qc/9607071.
[32] I. S. Booth and R. B. Mann, Nucl. Phys. **B539**, 267 (1999), gr-qc/9806056.
[33] O. J. C. Dias and J. P. S. Lemos, Phys. Rev. D **69**, 084006 (2004), hep-th/0310068.
[34] O. J. C. Dias, Phys. Rev. D **D70**, 024007 (2004), hep-th/0401069.
[35] J. Bičák and P. Krtouš, J. Math. Phys. **46**, ??? (2005), gr-qc/???
[36] P. Krtouš, in preparation.
[37] P. Sládek and P. Krtouš, in preparation.
[38] P. Krtouš, *Accelerated black holes*, web presentation at http://utf.mff.cuni.cz/~krtous/physics.